

The benzazole scaffold: a SWAT to combat Alzheimer's disease

Cite this: *Chem. Soc. Rev.*, 2013, **42**, 7747

Sabrina Noël,^{ab} Sarah Cadet,^{ab} Emmanuel Gras^{*ab} and Christelle Hureau^{*ab}

Neurodegenerative disorders including Alzheimer's disease (AD) are drawing scientists' attention within various fields, being one of the most serious diseases mankind will have to fight against in the very near future. AD is multi-factorial and is characterized by two histopathological hallmarks: the senile plaques made of amyloid- β ($A\beta$) peptide fibrils which also contain high levels of transition metal ions and the neurofibrillary tangles of Tau protein. $A\beta$ aggregation, possibly modulated by metal ions, is now considered as an important factor in AD aetiology. Hence, chemists are studying the details of molecular features at the origin of the disease with special interest in $A\beta$ aggregation and in the design of new molecules for the early diagnosis of AD or with curative properties. In this context, the benzazole molecular scaffold, included for instance in Thioflavin-T, an $A\beta$ fibril specific dye, or the **PIB** imaging agent, appears to be very attractive and exhibits multiple uses. In the present review, we have thus focused our interest on the applications of benzazole derivatives for understanding, diagnosing and curing AD. After having analysed the synthetic access to 2-arylbenzazoles, we have described a selection of recent applications of such compounds aiming to combat AD. They include the use of Thioflavin-T for the monitoring of $A\beta$ aggregation, the investigations of new PET and SPECT imaging agents for the detection of the senile plaques, the development of bi-functional molecules, encompassing the 2-arylbenzazole moiety for $A\beta$ binding and a chelating unit for metal ions coordination for instance.

Received 1st March 2013

DOI: 10.1039/c3cs60086f

www.rsc.org/csr

Key learning points

- Impact of the benzazole scaffold in various strategies (knowledge, diagnosis and therapy) to fight Alzheimer's disease.
- Description of efficient synthetic routes to 2-arylbenzazole molecules.
- A selection of the most efficient 2-arylbenzothiazole derivatives used in PET and SPECT imaging of senile plaques.
- Use of Thioflavin-T and neutral counterparts as *in vitro* agents for the monitoring of amyloidogenic peptide aggregation.
- Up to date report of bi-functional compounds, combining an amyloid- β binding moiety (from the 2-arylbenzothiazole scaffold) and either a metal chelation moiety or an acetylcholinesterase inhibitor moiety.

1. Introduction

1.1. Main molecular features of Alzheimer's disease

Alzheimer's disease (AD) is the most common cause of dementia in the elderly population accounting for 50 to 80 percent of dementia cases (www.alz.org). The worldwide prevalence of AD is approximately 30 million, a number that is expected to quadruple in the next 40 years. As a direct consequence, AD represents a global public health problem that will become even more important in the next few years.

An early symptom is the difficulty to remember newly learned information. Later on, more severe symptoms are encountered including mood and behaviour changes, confusion, serious memory loss, judgment alteration, and difficulties in speaking, writing and walking. Post-mortem neuro-histological hallmarks are extracellular amyloid plaques and intracellular neurofibrillary tangles of hyperphosphorylated Tau protein. It has been proposed that the apparition of the amyloid plaques (or senile plaques) is an early event that precedes, and thus likely induces, the hyperphosphorylation of Tau protein and the associated neuronal degeneration.¹ This is in line with the so-called amyloid cascade pictured in Fig. 1. According to this hypothesis, aggregation of the amyloid- β ($A\beta$) peptide is linked to the aetiology of the disease, since soluble monomeric forms are found in the healthy brain while amyloid plaques are

^a CNRS, LCC (Laboratoire de Chimie de Coordination), 205, route de Narbonne, F-31077 Toulouse, France

^b Université de Toulouse, UPS, INPT, LCC, F-31077 Toulouse, France.
E-mail: christelle.hureau@lcc-toulouse.fr, emmanuel.gras@lcc-toulouse.fr;
Fax: +33 (0)561553003; Tel: +33 (0)561333162

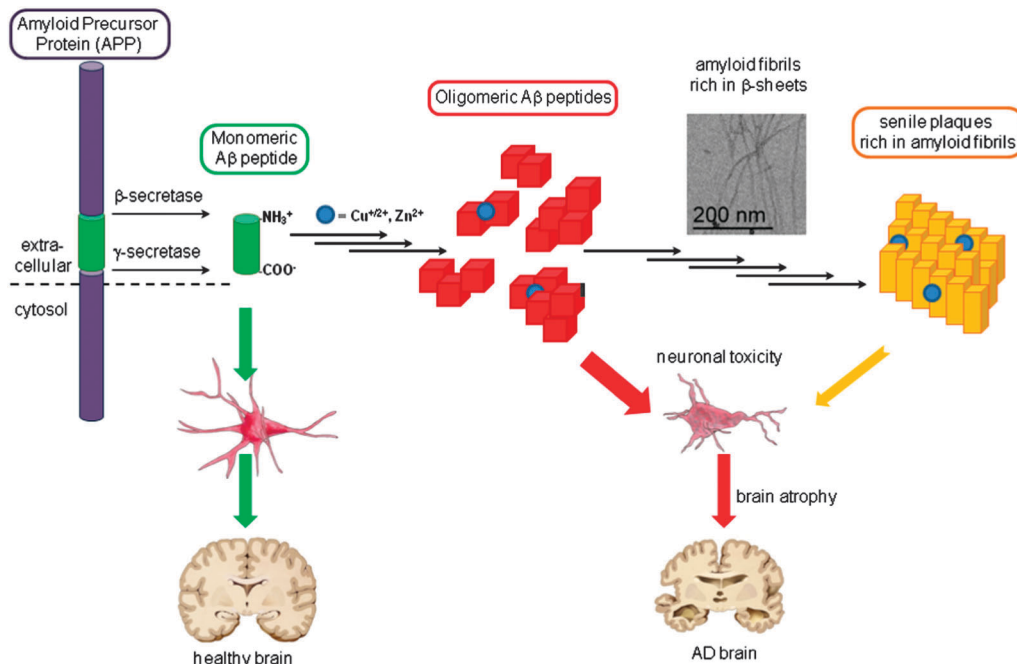


Fig. 1 The amyloid cascade process enhancing the role of metal ions. The A β peptide is obtained by cleavage of the Amyloid Precursor Protein (APP) by the β and γ secretases. The monomeric soluble A β is not neurotoxic (green arrow) and is found in healthy brains. The senile plaques are a post-mortem hallmark of the disease detected in AD brains. Intermediate species between the monomeric A β and the amyloid plaques are considered to be more toxic (red arrow) than the plaques themselves (orange arrow) leading to neuronal death and brain atrophy. Metal ions (blue circles) are considered as triggering agents of the aggregation process. Note that only the reactions resulting to the amyloid plaques are shown. However, all the reactions involved in this process are equilibrated ones.

detected in an AD patient's brain.^{2,3} These plaques contain amyloid fibrils of several microns in length and 7–12 nm in diameter, rich in β -sheets. Hence they can be imaged by PET/SPECT techniques associated with the use of radiolabelled molecules able to bind the β -sheet structure.⁴ Actually, intermediate species of the aggregation process, *i.e.* the oligomeric soluble forms of the A β peptides, are considered as the most toxic species, which disrupt synaptic function and the integrity of the membrane bilayers and lead to production of Reactive Oxygen Species (ROS).³ But, there is currently no efficient tool to detect oligomeric intermediates. In addition, metal ions were found in high concentrations in the amyloid plaques, leading to a modified amyloid cascade hypothesis in which metal ions modulate the aggregation of the A β peptide (Fig. 1).

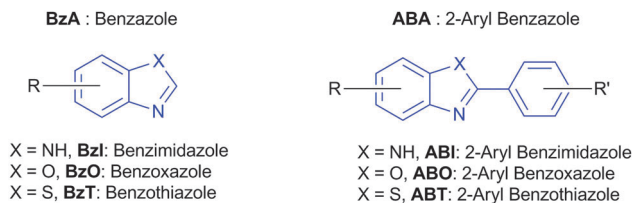
The A β peptide is a 39 to 43 residues polypeptide incorporating an N-terminal weakly structured hydrophilic part (residues 1–16) and a C-terminal hydrophobic part, which contains two β strand sequences (residues 17–21, known as the central hydrophobic core and residues 29–39/43). The N-terminal part is responsible for the binding of metal ions, mostly Cu and Zn, involved in modulation of A β aggregation properties and, for Cu, in ROS production.⁵

At present, the slowdown of the disease progression is hampered by the absence of curative molecules, *i.e.* drugs able to stop the neurodegenerative process. All the medications so far are symptomatic treatments tackling the consequences of the disease rather than the disease itself. In addition, the lack of physiological markers for the early diagnosis of the disease precludes both the administration of the symptomatic treatments

at the right time and the development of curative drugs. Last but not least, a thorough characterisation of the amyloid cascade process and in particular of the A β aggregation can help in the design of diagnostic and curative tools to fight AD. Interestingly, the 2-arylbenzothiazole (ABT) molecular scaffold is a very valuable tool used in these three aspects: (i) understanding of the amyloid cascade, (ii) developing new markers for the early detection and (iii) bi-functional curative molecules incorporating an ABT unit to target the A β aggregates and/or to impact A β aggregation. This explains why the use of the ABT scaffold as a building moiety has undergone a great development over the last few years in the AD field. This is illustrated by the constant increase of the citation numbers from almost zero in 2000 to more than 500 in 2012 (data from the ISI web of knowledge with “benzothiazole” and “amyloid” as topic key words).

1.2. The benzazole scaffold in therapeutics

ABT are members of the larger family of 2-aryl-benzazole (ABA) molecules, derived from the benzazole (BzA) entities. The chemical structure of ABA is constituted of an aromatic bicyclic system made of a 6-membered carbocycle fused with a 5-membered heterocycle incorporating one nitrogen and a second heteroatom (N for 2-aryl-benzimidazole (ABI), O for 2-aryl-benzoxazole (ABO) and S for 2-aryl-benzothiazole (ABT), Scheme 1), the position 2, between the two hetero-elements, bearing an aromatic substituent. As for the related biaryl compounds the two aromatic moieties are not co-planar in the ground state. Nevertheless the rotation around the σ -bond between them is less restricted in the case of ABA (compared to



Scheme 1 Nomenclature of the benzazoles and their 2-aryl derivatives used in the present review.

biaryl) due to the lower steric hindrance generated both by the 5 membered nature of one cycle and the lack of substitution on at least the sp^2 hybridized nitrogen neighbour. This makes the coplanar conformer more accessible allowing a larger electronic delocalization linked to the high potential ability of ABA to fluoresce.

Numerous benzazoles (BzA) in general and more particularly their 2-aryl derivatives (ABA) have been developed with a wide array of biological applications (Fig. 2), including brain therapeutics, evidencing the ability of these structures to cross the blood-brain barrier (ref. 6 and 7 and references therein). Numerous benzimidazoles (BzI) have also been developed to address the antibiotic resistance and these derivatives exhibit anti-bacterial, anti-fungal and anti-parasitic properties; ABI have more specifically generated significant interest in anti-cancer therapies. Similar activities have been reported for benzoxazoles (BzO) and benzothiazoles (BzT). BzT exhibit anti-inflammatory activities, as well as anti-diabetic, anti-parasitic, anti-oxidant and anti-convulsing activities. More specifically ABT also exhibit

anti-microbial activities and anti-cancer activities. However over the last few years one major field of application of these compounds has been the study of AD because of their ability to interact with $A\beta$ fibrils. Although a few ABI and ABO have been described for such applications,⁸ ABT remain the most developed compounds toward this goal.⁷ This trend can be mainly linked with the use of the well-known Thioflavin-T (ThT) as a neurohistological dye of amyloid fibrils.

In the present review, we will focus on the use of the ABT scaffold for understanding, diagnosing and curing AD (Fig. 2). We will first highlight the various synthetic routes giving access to the ABA scaffolds.

2. Syntheses of 2-arylbenzazoles (ABA)

2.1. Introduction

There are three main routes leading to ABA (Scheme 2). The first one (Scheme 2, path A), a linear strategy, classically consists of synthesizing the amidine, the amide or the thioamide and then performing a cyclization in order to generate the heterocyclic moiety. This can be achieved either *via* a classical aromatic electrophilic substitution or *via* a ring closure by formal displacement of a halogen or C–H activation. These approaches have been covered recently⁹ and are still a field of research efforts.¹⁰ The other two approaches are convergent ones and therefore more relevant for Structure–Activity Relationship (SAR) studies; one consists in building the BzA ring followed by a cross-coupling reaction which provides the ABA core

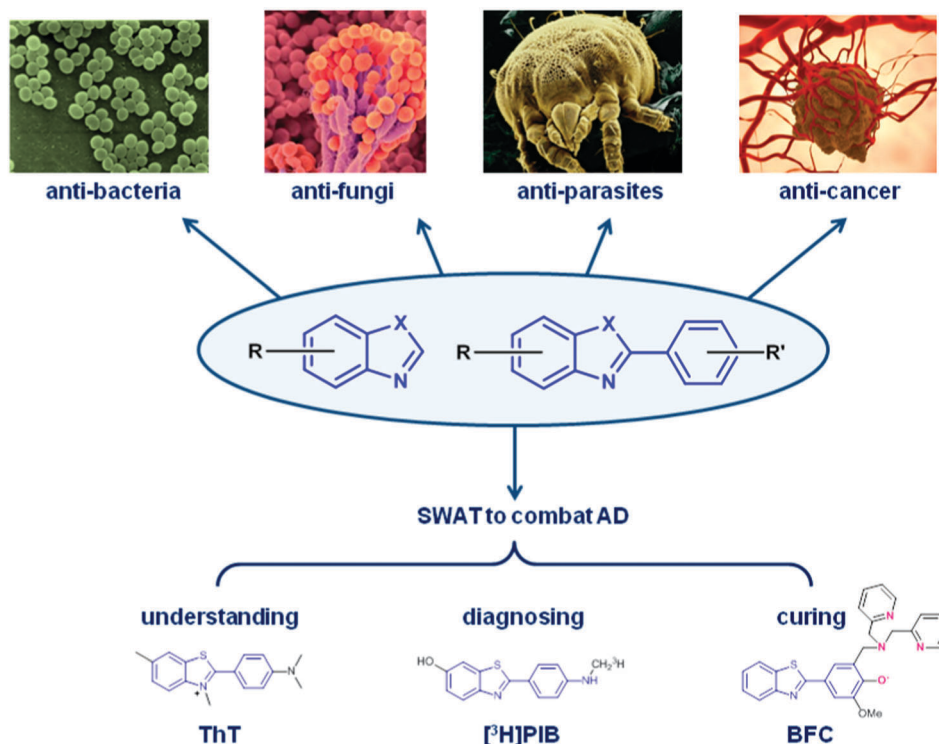
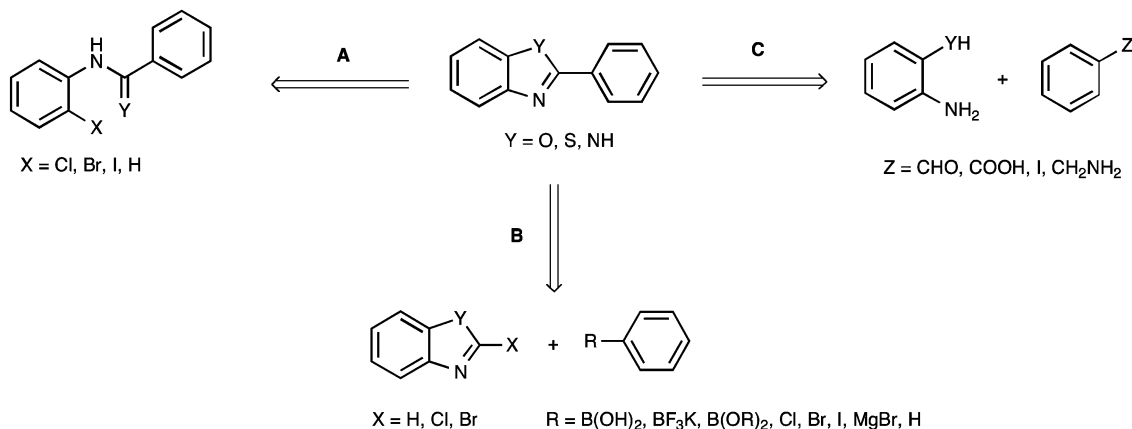


Fig. 2 Different biological activities of benzazole (BzA) and 2-arylbenzazoles (ABA) derivatives (top) and their uses in fighting against AD (bottom).



Scheme 2 Pathways leading to the 2-arylbenzazole (ABA) core.

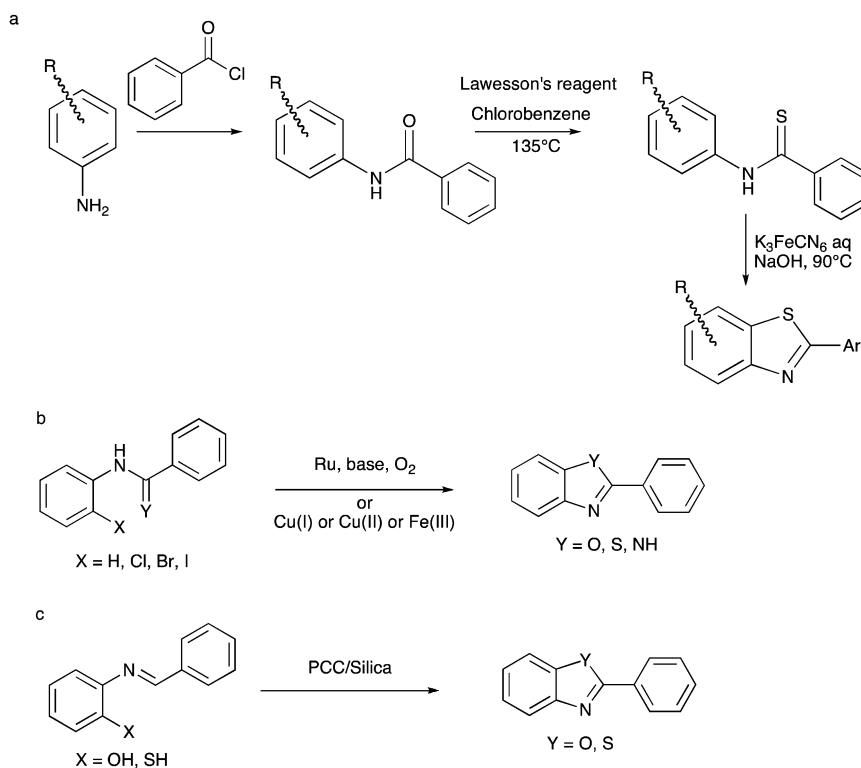
(Scheme 2, path B). In the last one (Scheme 2, path C) the heterocyclic ring of the ABA is accessed through the condensation of an aminophenol, aminothiophenol or phenylenediamine with an aromatic ring bearing reactive substituents, the nature of which depends on the operating reaction conditions. The three strategies can somehow be applied for ABI, ABO and ABT as indicated in the following schemes and we will in the text mainly focus on the most relevant target for each approach.

2.2. Linear strategy

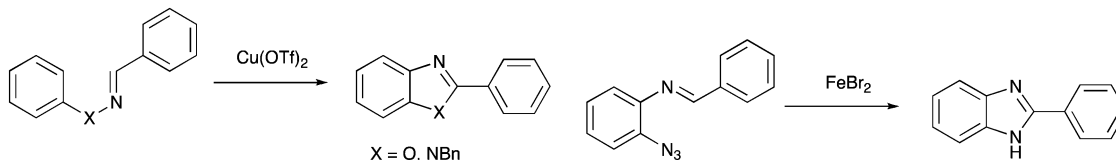
The linear approach has been thoroughly applied for the syntheses of ABT. The cyclization yielding the ABT is classically

performed using an oxidant (for example potassium ferricyanide) under Jacobson's conditions (Scheme 3a).⁹ However it must be pointed out that this classical cyclization is highly substituent dependent with yields varying from 25% to 75%. Due to the high availability of the starting material, it remains a competitive process for producing one derivative. Yet this oxidative strategy remains limited to the synthesis of ABT derivatives due to the very specific reactivity of sulphur toward oxidants.

Similar intramolecular cyclization methods (Scheme 3b, $X = \text{H}$) have been described from amides ($Y = \text{O}$), thioamide ($Y = \text{S}$) or amidines ($Y = \text{NH}$) under other oxidative conditions. One example is a photo-redox process to produce ABT,¹¹ a method



Scheme 3 Cyclisations in the linear approach: Jacobson's type cyclisation (a), C–H or C–X directed cyclisations (b) and Schiff's base cyclisation (c).



Scheme 4 Alternative linear approaches.

which although highly efficient (63 to 91%) does not tolerate photo-redox active functional groups such as nitro substituents. ABI have been accessed in high yields (68 to 89%) using homogeneous copper catalysis under an oxygen atmosphere.¹² This method has been found to be highly tolerant toward a wide range of functional groups, but has not been extended to the syntheses of ABO and ABT.

The cyclization to ABA can also be directed by the presence of a halogen at the *ortho* position to increase the selectivity of the reaction (Scheme 3b, X = Cl, Br, I). This reaction can be catalyzed by Cu(II), Cu(I) (ref. 13 and references herein), or Fe(III).¹⁴ A good efficiency is usually achieved by the copper catalysed methods regardless of the substitutions, contrasting with iron catalysis.

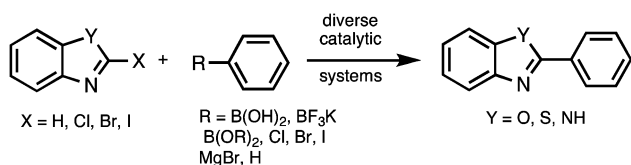
The cyclization can also be achieved from a Schiff's base (Scheme 3c) using pyridinium chlorochromate supported on silica, leading to ABT and ABO with good to excellent yields (74–91%).¹⁵

ABO and ABI have also been accessed in a similar linear approach *via* a Cu(II) catalysed rearrangement of oxime and hydrazones (Scheme 4).¹⁶ These rearrangements proved very general allowing a wide array of substitutions to be introduced on the 2-aryl moiety, but selectivity issues can be feared with unsymmetrically substituted arenes. ABI have also been accessed from the corresponding azides through Fe(II) catalysis.¹⁷

2.3. Coupling strategy

Although these linear approaches have shown a number of applications, it must be reminded that their application for SAR studies can become tedious. Therefore a convergent strategy based on cross-coupling might be favoured, since it allows efficient access to a wide array of compounds (Scheme 2, path B). Two types of coupling have been described in the literature: C–H activation and Suzuki-type coupling (Scheme 5).

Syntheses of ABA have been achieved by C–H activation using a boronic acid or a halide, catalyzed by palladium and copper.¹⁸ Microwave irradiation coupled with organometallic catalysis has also proved to be an efficient way to access these heterocycles.¹⁹ Xie *et al.* also showed that it is possible to use a carboxylic acid derivative in the presence of silver and palladium to generate ABO and ABT *via* a decarboxylative pathway.²⁰



Scheme 5 Coupling reactions leading to 2-arylbenzoxazoles (ABA).

This method has the advantage of having carbon dioxide as a by-product, facilitating the separation step. Even more atom economical, a direct arylation of benzoxazole has recently been reported to be achieved *via* a double C–H activation by Pd(II)/Cu(II) catalysis in good to excellent yields (52–94%).²¹ Although this approach is inherently appealing, the regiocontrol remains nevertheless limited.

A typical Suzuki–Miyaura reaction (SMR) between an aryl-boron species and 2-bromo-BzT in the presence of Pd(II) and Cu(I) has been shown to provide access to ABT derivatives with moderate to good yields.²² As an alternative to the SMR, the nickel-catalyzed Kumada–Corriu cross coupling has been successfully exploited to access ABO and ABT with good to excellent yields (74–99%).²³

2.4. One-pot reactions

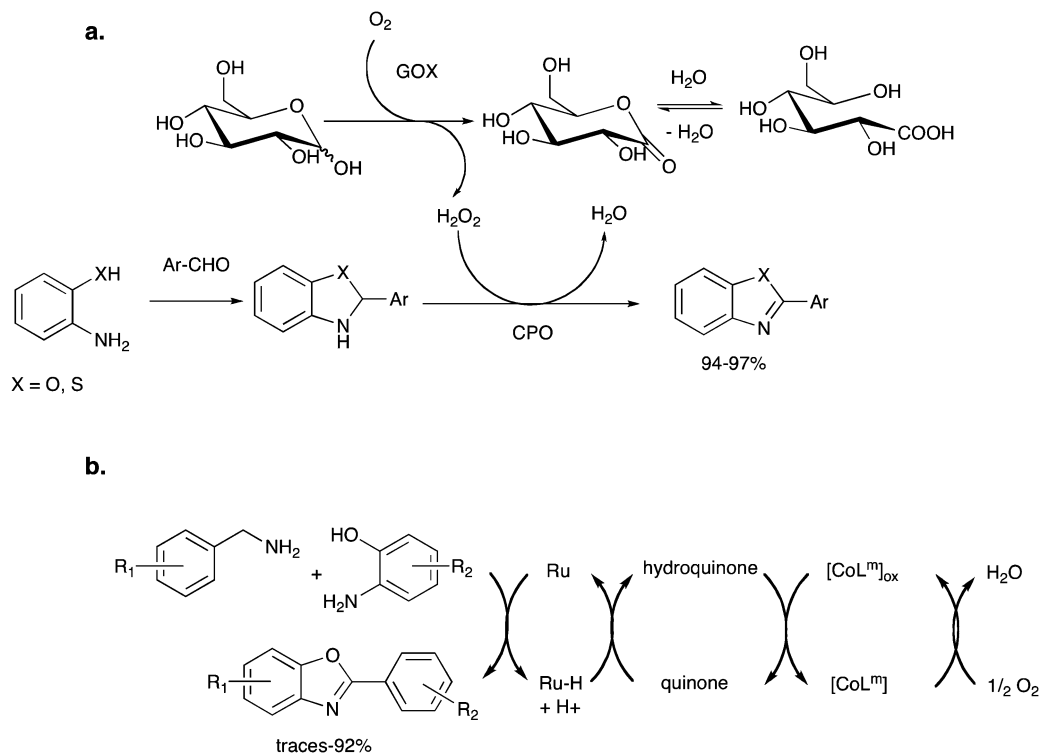
Finally, ABA can be synthesized by one-pot reactions classically by condensation of a 2-aminophenol, a 2-aminothiophenol or a 1,2-phenylenediamine derivative and a benzoic acid derivative. These reactions are carried out with Lewis acid activation and sometimes at high temperatures (ref. 24 and references herein). The benzoic acid derivative (Scheme 2, path C) can either be a carboxylic acid or it can be generated *in situ* starting from an aldehyde or from a halide under a CO atmosphere using a palladium catalyst.²⁵ Benzylamines can also be used in the presence of atomic sulfur and without a solvent and catalyst.²⁶ This method gives access to all kinds of ABA; however ABI appear to be preferred targets in terms of achieved yields (72–93%) regardless of the substitution pattern.

Finally two recent original methods also illustrate this approach. One based on the combination of glucose oxidase (GOX) and chloroperoxidase (CPO) has been used to produce hydroperoxide *in situ* (Scheme 6a).²⁷ This wide-scope method allows the synthesis of ABT and ABO in excellent yields (93–97%) under green conditions as water is both the solvent and the reaction by-product.

The second is a biomimetic oxidation, which has been reported using a Ru/Co catalytic system and benzoquinone as a co-oxidant. It converts benzylamine and aminophenol derivatives to ABO with varying yields (from traces up to 92%) mimicking the respiration mechanism (Scheme 6b).²⁸

2.5. Concluding remarks

We have highlighted here the main approaches yielding ABA. Although publications dealing with the synthesis of this scaffold are numerous (and have been thoroughly selected), one can mainly divide them into 3 categories. The first one, based on a linear synthetic approach, can be considered to be



Scheme 6 (a) Bi-enzymatic synthesis of 2-arylbenzothiazoles (ABT)/2-arylbenzoxazoles (ABO) in aqueous medium; (b) catalytic cycle of 2-arylbenzoxazoles (ABO) biomimetic synthesis.

of interest mainly when a single structure is targeted. SAR studies requiring a wider library of structures based on a similar scaffold are more likely to benefit from the more convergent synthetic approaches. Two classes of convergent methods can be distinguished. One is based on the construction of the azole ring from an *ortho*-substituted aniline, and therefore will be practically limited by the availability of the aniline (especially in the aminothiophenol series required to access the ABT derivatives). The second one is based on a cross-coupling reaction between a benzazole and an aromatic system. The development of methods based on C–H activation represents one major achievement for the synthesis of ABA as starting benzazoles are easily accessed, making this strategy perfectly adapted for both diversity driven approaches required for SAR studies and single target schemes. It must be pointed out that although the chemistry of benzazoles has been studied for ages, it has only recently evolved and is currently benefiting from state-of-the-art methods allowing it to stick to the current eco- and user-friendly requirements.

3. ABT scaffold: a tool for understanding AD

3.1. Thioflavin T: *in vivo* and *in vitro* staining of amyloid fibrils

The 2-arylbenzothiazole (ABT) derivative Thioflavin T (ThT) (Fig. 3A) is the most widely used staining dye for amyloid fibrils. Its first use as a histological marker of amyloids was reported in 1959 by Vassar and Culling, who demonstrated the potential of fluorescent microscopy for detection of fibrils. They described

the use of ThT as a potent fluorescent marker of amyloids with a selective localisation of ThT to amyloid deposits.²⁹

Later, due to its water solubility and to its correct affinity for fibrils (in the low μM range), the ThT dye was used for *in vitro* purposes, mainly to monitor the aggregation process of peptides leading to the formation of amyloid fibrils by fluorescence (Fig. 3B). Indeed ThT fluorescence yield is strongly enhanced when ThT is bound to fibrils. The characteristic fluorescence enhancement (about one to three orders of magnitude) of ThT upon binding to fibrils is proposed to arise from the preclusion of the free rotation between the di-methyl aniline and BzT rings. Indeed, the free rotation of the two moieties about their common carbon–carbon bond that exists in solution (Fig. 3A) leads to the change from the locally excited (LE) state to a non-radiative charge transfer state and thus to low emission. When bound to fibrils, such rotation is partially hampered leading to a more populated LE state responsible for a higher fluorescence yield.³⁰ In addition to fluorescence enhancement, ThT displays a dramatic bathochromic shift of the excitation and emission maxima when bound to fibrils (from 385 nm to 450 nm and from 445 nm to 480 nm, respectively).^{29,31}

A typical sigmoid curve observed for amyloid fibrils formation by ThT fluorescence is shown in Fig. 3B. In the beginning of aggregation, the low ThT fluorescence indicates a nucleation phase where the peptides are under the forms of monomers or low molecular weight oligomers with no β -sheet content. The steep increase of the ThT fluorescence corresponds to the elongation phase during which protofibrils rich in β -sheets are formed. When the equilibrium between the

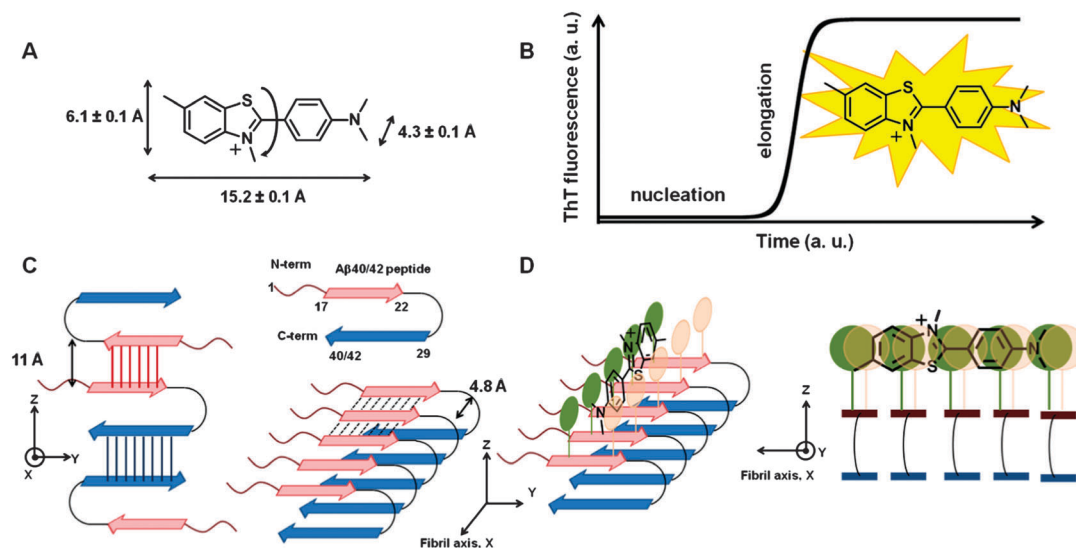


Fig. 3 (A) ThT dye with its specific dimensions. (B) Sigmoid ThT fluorescence curve observed for the formation of amyloid fibrillar aggregates containing β -sheets. (C) Scheme of A β peptide; β -sheets interactions along the z axis involve side chains of the amino-acids residues (left) while β -sheets interaction along the x axis (fibril axis) involves H-bond between backbone CO and NH groups (right). (D) Scheme of ThT interaction within the fibrils along the fibril axis (left) and perpendicular to it (right). Green and orange circles stand for hydrophobic residues (such as Phe, Leu, Val from the central hydrophobic core of A β peptide, see Section 3.2.) able to interact with aromatic rings of the ThT.

fibrils and the other states (monomers, oligomers, aggregates. . .) is reached, a plateau of the ThT fluorescence is obtained.² While ThT fluorescence is the most commonly used method to study aggregation processes and effect of aggregation inhibitors, some limitations have to be taken into account (see ref. 32 for a recent review). They include possible interference of ThT with the aggregation process itself, dependence of ThT fluorescence on the type of fibrils and the experimental conditions (pH, solvent. . .), self-quenching of the ThT fluorescence when used in too large concentrations. . .

3.2. Interaction of thioflavin T with A β fibrils

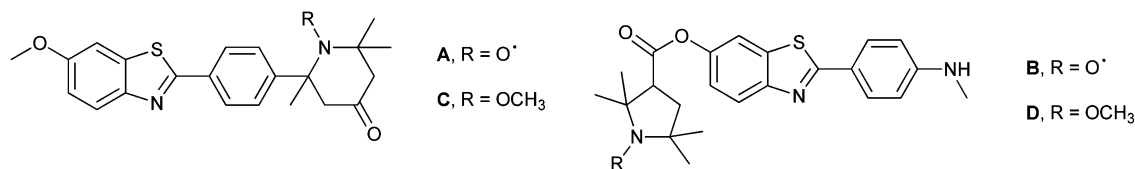
In addition to the previously mentioned limitations, ThT fluorescence suffers from a lack of specificity for a given amyloidogenic peptide (A β in the case of interest here, Fig. 3C). In other words, ThT cannot strongly distinguish between several amyloid fibrils from different peptides/proteins (α -synuclein, prion proteins, *etc.* . .). This is due to common structural features shared by these peptides/proteins, *i.e.* their organization in β -sheet structures.

The exact site of interaction of ThT with A β fibrils is still under debate, but several general trends have emerged which lead to the model proposed in Fig. 3D. ThT is aligned along the fibril axis (x) and inserted into hydrophobic grooves formed by the side chains of residues from the central hydrophobic core of the A β peptide (LVFFA). π -stacking interactions with aromatic residues (Phe) also contribute to the location of the ThT inside the hydrophobic grooves, leaving the dye in a blocked flat conformation, in adequacy with its fluorescence properties in fibrils. It was also proposed that five consecutive hydrophobic or aromatic residues are required for the ThT binding, in line with a 1 : 4 to 1 : 35 ThT : A β monomer ratio detected in A β fibrils.²⁹

The same site has been proposed for neutral analogues of ThT, which exhibit higher affinity for the fibrils (about one to two order(s) of magnitude).³¹ Neutral ThT analogues have mainly been developed for *in vivo* imaging (see Section 4).

3.3. New detection techniques for the monitoring of A β aggregation by ABT derivatives

Recently, new techniques have been used for *in vitro* monitoring of A β aggregation to overcome some of the limitations of the classical ThT fluorescence assay. They include electrochemistry of the BTA molecule (Fig. 5) used to monitor the aggregation of the murine A β 40/42 peptides. It was shown that the decrease in the electrochemical response of the BTA compound, due to its insertion in A β fibrils and thus to a slower diffusion to the electrode, correlates with the increase of BTA fluorescence in the control experiment.³³ Also microdialysis equilibrium was developed to characterize the interaction of ThT with various amyloid fibrils (including A β 42 fibrils). In contrast to ThT fluorescence, such methods allow us to determine binding parameters (stoichiometry of ThT : peptide and binding constants) and spectroscopic features of the bound ThT with no risk of erroneous interpretation.³⁴ Lastly, two nitroxyl radical derivatives (compounds A and B, Scheme 7) have been obtained³⁵ that can be (i) directly used in EPR (Electron Paramagnetic Resonance). Indeed, when inserted in A β fibrils, the free motion of the radicals is slowed down and this leads to a strong broadening of the EPR signals and (ii) potentially used for the detection of radical generation within the A β fibrils. Indeed, the nitroxide radical can quench the fluorescence of the compound, which is thus recovered when the radical is lost due to electron exchange reactions. It was shown that the latter effect can only be observed in compound A because in B no



Scheme 7 ABT derivatives integrating a nitroxide radical (**A** and **B**) and neutral counterparts (**C** and **D**).

fluorescence quenching is observed (fluorescence of **A** and **B** was compared to the fluorescence of the neutral methoxy counterparts, compounds **C** and **D**, respectively, Scheme 7). In addition, **A** and **B** show distinct properties in A β aggregation with **A** promoting it and **B** limiting it, effects that were attributed to the presence of the radical since **C** and **D** don't impact the aggregation process.

4. ABT scaffold: a diagnostic tool for AD

4.1. Generalities

Diagnosis of AD is currently based on clinical evaluation and patient history, combined with brain atrophy measurements by Magnetic Resonance Imaging (MRI).³⁶ This diagnostic methodology has proved to be quite efficient in moderate to severe stages of the disease, but is not able to detect the early phases of the pathology, brain atrophy being the evidence of advanced neurodegeneration. As neurodegeneration remains an irreversible process, it appears obvious that the early detection of histopathological lesions is an indispensable requirement in order to tackle the disease. Nevertheless these clinical and MRI assessments are the only diagnostic tools available to date; moreover the only way to confirm the pathology is by post-mortem examination of brain sections, and more specifically the identification of senile plaques and neurofibrillary tangles. These neuropathological hallmarks of AD are detected by way of ThT staining. From this statement and in order to achieve the early diagnosis of AD, the quest for sensitive non-invasive detection of these plaques has become an area of intense

research efforts. Among the imaging agents that are currently under investigation, a wide range of molecular probes are obviously derived from the ThT dye. As non-invasive methods require detection from outside of the body (especially in the case of AD outside the brain and the skull) the use of γ -rays becomes obvious and has driven this research toward nuclear imaging techniques such as Positron Emission Tomography (PET) and Single Photon Emission Computed Tomography (SPECT). This implies that the molecular probes have to be labelled with radionuclides (radiolabelled probes) which upon radioactive decay emit a positron (β^+ , antimatter of the electron) for PET imaging, or a γ photon (*via* electron capture for proton rich nuclides or isomeric transition for metastable nuclides) for SPECT imaging. Although these two techniques exploit the radioactive decay of a nuclide, they differ slightly as outlined in Fig. 4.

4.2. PET and SPECT specificities

PET imaging is based on the emission of a positron from the nuclide. This positron has a specific kinetic energy (which depends on the nature of the nuclide, and its half-life time) which allows it to travel along its mean free path until it undergoes an annihilation reaction with an electron from the surrounding matter (making it an ionizing radiation). This annihilation reaction produces two γ -rays emitted simultaneously in opposite directions. The detection of these two γ rays of 511 keV within a short timeframe on opposite sides of a circular array of detectors is indicative of the position of the annihilation event, and therefore of the presence of the

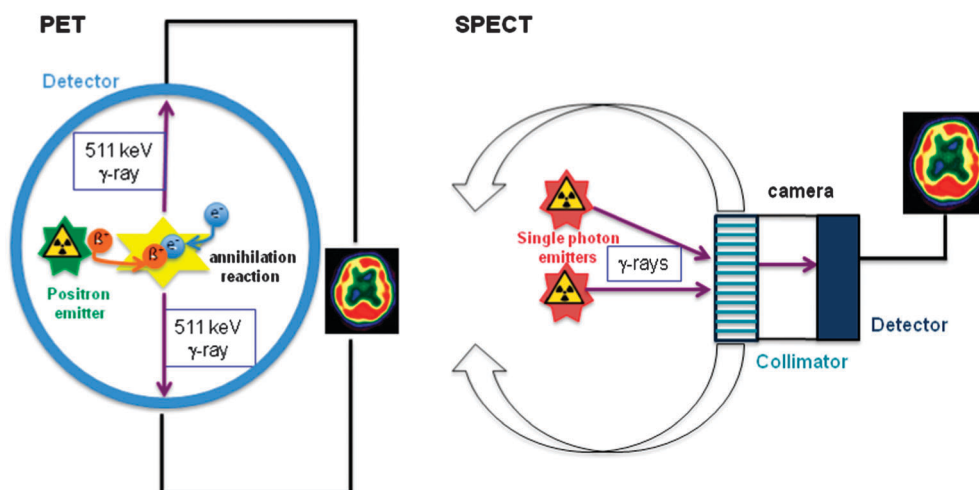


Fig. 4 PET and SPECT principles: comprehensive detection *via* a fixed camera (PET) vs. direction-selected detection *via* a rotating camera (SPECT).

Table 1 Some radioisotopes used in PET imaging and their main physical properties

β^+ -emitting isotope	^{15}O	^{13}N	^{11}C	^{18}F	^{68}Ga	^{62}Cu	^{64}Cu
Physical $t_{1/2}$ (min)	2.04	9.96	20.38	109.74	68	9.6	762
β^+ -energy (keV)	1723	1190	961	635	1940/920	2910	656
Radioactive decay purity (%)	99.9	100	99.8	96.9	89	98	19

^{123}I , $^{99\text{m}}\text{Tc}$ (m stands for metastable), ^{67}Ga and ^{111}In are γ emitters typically found in nuclear medicine services (used in SPECT).

radionuclide in the vicinity of this position. SPECT imaging is based on the radioactive decay of a nuclide which takes place with emission of a γ photon (energy of which depends on the nature of the nuclide). This photon is then eventually detected by a γ camera after going through a collimator. The rotation of the camera around the patient allows the identification of the areas of emission. In both cases, a picture reconstruction is computed in order to obtain a 3D view of the nuclide distribution. One advantage of PET relies on the comprehensive detection of the annihilation events, allowing a quantitative measurement to be carried out. Its drawback is related to the mean free path of the positron which induces a loss of resolution.

There is a range of positron emitting nuclides which are commonly used or gaining increasing interest, including ^{15}O , ^{13}N , ^{11}C , ^{18}F for organic molecules and ^{68}Ga , $^{99\text{m}}\text{Tc}$ for inorganic complexes (Table 1). Among them ^{18}F appears clearly as the most suitable one for labelling small molecules as its size does not strongly modify the overall shape of the molecule. Cu and Ga are less ideal for this purpose since they need to be coordinated. Their requirement for a ligand will thus significantly modify the molecular structure (unless the molecule features a chelating part, see for instance the “integrated approach” Fig. 5).

The radiosynthesis of A β probes has been recently reviewed and will not be discussed in detail here.³⁷ As stated from the nature of the element quoted, one can see that radiolabelled molecules can either be organic molecules or metal complexes. The advantage of the former is their potential *in vivo* stability (covalent bonding would not suffer from potential *in vivo* metal exchange with biomolecules exhibiting a high metal affinity), whereas the advantage of the latter lies in the ease of access by simple complexation which can be carried out in water as the final step (less time consuming than more sophisticated synthesis).

4.3. Molecular requirements for PET and SPECT imaging

We will focus more on the basic requirements for suitable PET and SPECT imaging agents in AD. This includes good penetration of the blood–brain barrier (BBB), selective binding to A β plaques, and clear and contrasting signals between plaque and non-plaque interactions (signal to noise ratio). As previously mentioned, the ThT has provided an interesting entry for the development of these agents since its low molecular weight allows it to fulfil one of the requirements of Lipinski’s rules: (i) less than 5 H bond donors; (ii) less than 500 Da molecular weight; (iii) log P less than 5; less than 10 H bond acceptors. Moreover, its molecular structure allows the introduction of chemical modifications by substitutions in its aromatic rings,

either on the BzT side or on the 2-aryl moiety. Since significantly lipophilic derivatives were necessary to achieve a good BBB crossing it appeared to be necessary to remove the positive charge found in the ThT structure which yielded a number of ABT derivatives. The disappearance of the charge has been correlated with a significant increase of the binding affinity for fibrillar A β aggregates. Moreover ^{11}C labelling showed evidence of the ability of these compounds to readily enter the brain.³⁸ From this initial finding, many analogues of the ABT scaffold have been synthesized and evaluated as imaging agents. Table 2 lists some of the most effective analogues described in the literature as A β imaging agents, taking into account their lipophilicity, their penetration in and rapid clearance out of healthy brains, their affinity for A β fibrils and in some cases their selectivity for A β plaques.

4.3.a. Lipophilicity. The lipophilicity reflects the tendency of a molecule to accumulate in biological membranes of living organisms. This physical characteristic is evaluated by the log P (partition coefficient), which is the ratio of the concentration of the compound in octanol *versus* its concentration in water at pH 7.4. The optimal range of log P for brain penetration lies between 1 and 4. Thus, the compounds developed to obtain such a value must still exhibit a moderate hydrophilic character. This can be achieved if the designed compounds exhibit an ability to form hydrogen bonds. Toward this goal, hydroxy or N-substituted amino group have been frequently used to decorate the A β targeting probes (see Table 2). Moreover, the protonation state ($\text{p}K_{\text{a}}$) of these functions can play a dramatic role in the lipophilicity of the compound. This tends to restrict the choice of the nature and the number of their substituents and neighbouring groups. Generally speaking, this trend has a significant influence on the optimal positioning of the radioisotope either on the 2-aryl part or on the BzT part of the molecule. Recently, in order to prevent these limitations and to allow a better modulation of the hydrophobic balance the insertion of an ethylene glycol moiety (PEG unit) has been carried out to introduce the radioisotope without impacting the *in vivo* properties of the molecule (Table 2, entry 2).

4.3.b. Determination of *in vitro* A β binding affinity. The *in vitro* determination of the binding affinity of the ligands is typically carried out using two different assays, based either on fluorescence or radioactivity. The fluorescence method is based on the observation that some ligands exhibit a significant change of their fluorescence properties upon binding with A β fibrils. Typically, the ThT fluorescence shift is used to measure the binding affinities of competing ligands. However, *in vitro* binding assay based on radioligand titration is another approach of interest as it allows testing the compounds against

Table 2 Imaging agents designed from the ABT scaffold

Entry no	Structure	log <i>P</i>	Affinity for Aβ, <i>K</i> _i (nM)	Brain penetration, %ID per g	Brain washout %ID per g	Selectivity	Ref.
1		3.20 ± 0.06	5.5 vs. [³ H]PIB	6.62	0.73	Selective binding to Aβ plaques	39
2		2.4	7.2 vs. [¹¹ C]BTA-1	10.3	3.8	Selective binding to Aβ plaques	
3		2.1	> 600	10.3	2.8	n.d.	40
4		n.d.	>600	n.d.	n.d.	n.d.	
5		2.48 ± 0.063	11.5 ± 3 [¹²⁵ I]IMPY	4.3	0.09	binding to Aβ plaques	41
6		1.35 ± 0.01	3.8 vs. [¹¹ C]PIB	10.2	0.96	n.d.	
7		2.93 ± 0.02	8.4 vs. [¹¹ C]PIB	12.5	1.98	n.d.	42
8		2.81 ± 0.02	3.4 vs. [¹¹ C]PIB	19.3	1.96	n.d.	
9		2.29 ± 0.24	2.2 ± 0.5 vs. [¹²⁵ I]IMPY	5.1	0.43	n.d.	43
10		2.52 ± 0.27	5.7 ± 1.8 vs. [¹²⁵ I]IMPY	5.33	0.27	n.d.	
11		2.7	11	0.4	0.057	Selective binding to Aβ plaques	
12		3.1	10	0.22	0.083		44
13		1.2	4.9	0.33	0.10		
14		2.5	4.3	0.21	0.018		
15		3.17	8.32 vs. [³ H]BTA-1	9.08	3.4 (30 min)	n.d.	
16		n.d.	7.1 [³ H]BTA-1	7.76	2.66 (30 min)	Selective binding to Aβ plaques	45
17		1.65	11.1 vs. [³ H]BTA-1	5.64	0.36 (30 min)	n.d.	
18		2.35	3.22 vs. [³ H]BTA-1	7.76	2.66 (30 min)	n.d.	45

This also raises some concerns about the worldwide reproducibility of the affinity measurements, and prompts us to consider that the absolute values should only be handled and

compared carefully. This is evidenced by a comparison of entries 5 and 6 in Table 2 for which different values are obtained for the same compound. It should therefore simply

be accepted that a radioligand can be considered as a good competitor when its affinity for A β species is in the nanomolar range.

As illustrated in Table 2, the compounds developed so far should not exhibit sterically demanding groups on the 2-aryl ring. We have shown that the substitution of the 4' position of this ring with an NHMe group leads to optimum affinity in a series of ABT derivatives, and that the replacement of the methyl by a bulkier group induces a decrease of the binding affinity.²⁴ It can be further observed that the introduction of a side chain on the 2-aryl ring strongly affects the affinities toward A β (Table 2, entries 3 and 4 *versus* entry 2). However when these substitution patterns are avoided, the affinities of these derivatives are all measured *in vitro* in the nanomolar range.

4.3.c. BBB crossing. Another parameter of major interest is the ability of these chemical entities to cross the BBB. To assess this brain penetration, radio-labelled derivatives are injected into young, wild type mice that do not exhibit amyloid deposits in their brain. After injection of the radioligand, the mice are anesthetized and killed after a short period (typically 2 min post-injection). After brain excision and dissection, the samples are weighted and their radioactivity is measured in a γ counter to determine the percentage of injected dose per gram (%ID per g). A good brain penetration is achieved when within 2 minutes after injection the brain uptake is in the range between 3.3 and 16.6 %ID per g. The entry in the brain is strongly connected to the lipophilicity–hydrophilicity balance (indicated by the log *P* value) and the charge of the molecule (by *in vivo* protonation of the basic sites). It is therefore not surprising that this feature usually correlates with log *P* (Table 2).

The washout of the radio-labelled probe from the brain is performed similarly by sacrificial experiments carried out 30 min or 60 min after injection. These values are here expected to be low %ID per g. Indeed large values would be indicative of a healthy brain capture, and therefore would indicate a lack of selectivity of the compounds for the A β fibrils (*i.e.* strong interactions with other substrates in the brain which would at least negatively impact the signal to noise ratio).

4.3.d. Selectivity for amyloid plaques. Finally the specificity of the compounds for amyloid plaques in AD brain is carried out by fluorescence tissue staining experiments or autoradiography microscopy, depending on the fluorescence properties of the ligand. In fluorescence experiments, brain sections obtained from transgenic mice or from post-mortem brain of AD patients are stained with amyloid specific fluorescent dyes. The ligand is incubated under the same conditions. If the imaging agent has an appropriate fluorescence, the fluorescence patterns of the brain sections can be directly compared. If the same spots are revealed in the two experiments (with the amyloid specific dye and with the ligand) then the ligand can, to some extent, be considered as specific for amyloid fibrils. When the ligand lacks the required fluorescence properties, a radio-labelled version of the ligand is used. The autoradiographic picture is then compared with that obtained using fluorescence microscopy with the amyloid specific dye. Again a

correlation between the spots on the autoradiographic picture and the fluorescent spot might be indicative of a good specificity. It must be pointed out that the availability of brain sections can be scarce and therefore these measurements are not systematically carried out. Moreover such assays only provide a macroscopic picture of the spot of interaction, and might not be considered as strong evidence of selectivity for A β fibrils at a molecular level, but mainly as evidence of co-location with A β fibrils.

4.4. Best compounds

Based on these experiments, we have shortlisted some ABT derivatives which exhibit the most interesting features for *in vivo* imaging (Table 2). Most often, these compounds are efficiently delivered into the brain and they can mainly tolerate substituent variations (especially introduction of a larger substituent, entry 2 in Table 2) on the BzT part of the ABT.

To date, Pittsburgh's compound ([¹¹C]PIB, Fig. 5) has been one of the most extensively tested radio-labelled probes for PET imaging of the A β load in the brain of AD patients. Although its specificity for A β fibrils is still questioned,⁴⁶ fluorinated derivatives of PIB have also been reported, since due to the short half-life time of ¹¹C (20 min, Table 1) [¹¹C]PIB is far too restricted to a few PET centres featuring the required facilities. Oppositely fluorinated analogues (110 min, Table 1) represent a promising alternative that can be delivered over long distances (as it has been shown with [¹⁸F]-fluorodesoxyglucose).⁸ Flutemetamol is a fluorinated analogue of PIB currently in advanced clinical trial. Although not an ABA structure, one might also consider the singular structural similarity of AZD4694 (also known as NAV4694, currently in clinical trial) with the ABA moieties (Fig. 5).

4.5. Bi-functional imaging agents with ^{99m}Tc

In addition to purely organic imaging agents (IA), some BFIA (Bi-Functional Imaging Agents) based on an ABT moiety linked to a ^{99m}Tc chelator have also been developed, although with moderate success (Fig. 5) (ref. 4 and references therein). This is mainly due to a very low brain uptake, caused either by poor metabolic stability (2 in Fig. 5), or to negatively charged complexes (3 in Fig. 5). In contrast, compound 1 has a good brain uptake and its Re analogue shows fluorescence staining consistent with A β fibrils binding. More recently, a large series of promising Re surrogates (4 and 5 in Fig. 5) have been synthesized using an integrated approach, with the aim of decreasing the molecular weight.⁴⁷ They exhibit good to moderate affinity for A β fibrils *in vitro* and still have to be tested with ^{99m}Tc *in vivo*.

5. ABA: a therapeutic tool

5.1. Study of ThT impact on pathological features related to A β peptide aggregation

In a recent study, it was shown that ThT and neutral analogues (HBX, HBT, Fig. 5) were efficient in extending the lifespan and healthspan of adult nematodes, with HBX and HBT being active

at much lower concentration than ThT (1 μM versus 50 μM).⁴⁸ Several mechanisms were tested to explain such an effect. Retained mechanisms include improved protein homeostasis induced by ThT and ability of ThT and ABT derivatives to interact with aggregating proteins leading to a proper folding. In parallel, it was shown that ThT can reduce aggregation of the A β 3-42 [note that A β 3-42 corresponds to the A β 42 peptide lacking the first two amino-acid residues, which has a higher aggregation propensity than the full-length A β 42 peptide] responsible for worm's paralysis, and can also decrease the levels of soluble oligomers and co-localize with A β aggregates *in vivo*. These results provide evidence for positive effects of ABT derivatives in age related diseases including AD.

5.2. ABA derivatives as A β binding moieties in bi-functional chelators (BFC)

As shown previously, the ABT moiety has some propensity to inhibit A β aggregation *in vivo*. In addition, a deleterious impact of metal ions in the amyloid cascade linked to the aetiology of AD has been proposed (see Section 1.1). Hence, one recent strategy relies on the development of Bi-Functional Chelators (BFC) combining the two potentially therapeutic functions. It has to be noted here that a similar strategy has also been applied with other moiety for A β binding, including stilbene derivatives and **IMPY** (Fig. 5) derivatives.⁴⁹ As for the BFA, two approaches have been tested with the metal chelator embedded to the ABA part (integrated approach, Fig. 5) or linked to it (1 + 1 approach, Fig. 5). Several positive effects are expected from the combination of the two A β binding and metal chelators entities: (i) potentiating the effects of the two entities; (ii) improving brain penetration of the chelators; (iii) increasing the specificity for A β ; and (iv) thus reducing side-effects such as disturbance of metal ions homeostasis and normal functions of essential metallo-enzymes.

Several compounds have been developed in this direction (Fig. 5, Table 3). The first reported BFC, the **XH1**, was made by two neutral ABT linked by amide bonds to a central diethylenetriaminetriacetic core as the chelating moiety. **XH1** reduces Zn(II)-induced A β 40 aggregation *in vitro* and reduces APP expression in human SH-SY5Y neuroblastoma cell lines. It also attenuates A β pathology in transgenic AD model mice after a

four week period without apparent neurotoxicity at low μM concentrations.⁵⁰

More recently, BFC combining other chelating units based on amino-pyridine ligands (Fig. 5) were reported.^{51,52} The **FC1** compound is able to exhibit high fluorescence in the presence of A β 40 fibrils, to penetrate the cell membrane, to inhibit Cu and Zn induced A β 40 aggregation and to partially solubilise Zn and Cu-A β 40 aggregates *in vitro*.⁵² The latter property was linked to the increased cytotoxicity induced by **FC1** on the neuronal cellular model, in line with oligomeric forms being more toxic than fibrillar aggregates (see Section 1.1. and ref. 3). Similar observations were made for the **L¹** and **L²** BFC for which the investigations were conducted with the more aggregating A β 42 peptide. However, in contrast to what was observed for **FC1**, for which the disaggregation of A β fibrils was only partial, in the **L¹** and **L²** cases, the Zn and Cu-A β 42 fibrils were efficiently disassembled into non-fibrillar aggregates and oligomeric species, respectively. The more efficient disaggregation propensity of **L¹** and **L²** BFC compared to **FC1** thus follows the Cu and Zn affinity of the chelating moieties (Table 3). In addition, the **L¹** and **L²** affinity for A β 42 was quantitatively determined using the intrinsic fluorescence (**L¹**) or by competition with ThT (**L¹** and **L²**). The compounds have a 10-fold (**L¹**) and 50 fold (**L²**) higher affinity for A β 42 fibrils than ThT. Impact of **L¹** and **L²** on apo-A β 42 fibrils solubilisation was also demonstrated. Lastly, both **L¹** and **L²** lead to a partial inhibition of H₂O₂ production by Cu-A β 42 under reducing conditions, with **L²** being more potent than **L¹** (>90% versus >65% inhibition).⁵¹

In the integrated strategy, the lead compounds are **HBXI**, **HBTI** and **BMI** (Fig. 5), where the chelator moiety is made of a phenolate oxygen and a sp² hybridized nitrogen atom is incorporated into the ABA structure, leading to the formation of 1 : 2 metal : ligand complexes. They were selected by an *in silico* procedure to have the BBB penetration propensity. Their Zn and Cu chelating abilities were determined (Table 3). They are close for Zn and follow the order **HBXI** > **HBTI** > **BMI** for Cu, which is in line with the Cu-A β 40 inhibition propensity determined by a crude turbidimetry assay. Regarding Zn, **HBTI** was the most efficient BFC. In contrast to **L¹** and **L²**, the effect of the compounds themselves was not observed on aggregation of the apo-peptide.⁵³

Lastly, some BFC were reported that combine the BzT scaffold and either a Schiff base (**XSABT**, Fig. 5)⁵⁴ or a deferiprone (**L₅**) motif.⁵⁵ They form 1 : 2 metal : ligand complexes with moderate and high affinity for Cu, respectively (Table 3). **XSABT** were shown to inhibit Cu-induced A β 40 aggregation and to decrease preformed Cu-aggregates. The Cu-complexes were also potent in preventing apo-A β 40 aggregation. In addition, **XSABT** diminish moderately the *in vitro* H₂O₂ production and the *in cellulo* ROS production, while protecting partially cells confronted with Cu-A β 40 induced toxicity.⁵⁴ Analogues of the **L₅** ligand were shown to possess intrinsic anti-oxidant properties and they were able to solubilize Cu-A β 40 aggregates with the same efficiency as the deferiprone moiety but were less efficient for Zn-A β 40 aggregates suggesting a metal specific effect.⁵⁵

Table 3 Affinity of Cu(II) and Zn(II) BFC. $\text{pM} = -\log[\text{M(II)}]_{\text{free}}$ with $[\text{ligand}]_{\text{total}} = 50 \mu\text{M}$ and stoichiometric metal concentrations. pM represents the Cu(II) or Zn(II) affinity of the ligand, with a higher figure corresponding to a higher affinity. See the ligand scheme in Fig. 5

	pH 6.6		pH 7.4		Ref.
	Cu	Zn	Cu	Zn	
L¹	9.6		10.4	8.0	51
L²	7.0		7.9	7.3	51
FC1			6.8	6.0	52
HBXI	11.1			11.0	53
HBTI	10.5			10.9	53
BMI	9.5			10.5	53
XSABT			5.9		54
L₅			~9		55

These BFC based on the assembly of the chelator unit with the ABA moiety show interesting results in metal induced A β damage. However, it seems that disassembling A β fibrils induces more cytotoxicity due to the formation of oligomeric intermediates,^{51,52} in line with the higher toxicity of the latter species reported in the literature.³ Hence a special effort to target the oligomeric species and/or to solubilise the fibrils into monomeric non-toxic forms remains to be made. A possibility includes modification of the ABA scaffold and for instance linking the chelator to the BzA side instead of the 2-aryl side. While such a possibility has been investigated in the case of the BFIA, it has still been ignored for BFC. Another point to note is that all the chelating moieties designed currently are well-suited for dicationic Cu and Zn ions. Cu(I) can also be an interesting target ion, due to the *in vivo* redox cycling of Cu.⁵ Last but not least, the brain delivery of such bi-functional compounds is a key parameter to account for. While low-molecular weight BFC fulfilling Lipinsky's rules are anticipated to enter the brain by passive diffusion,⁵³ more bulky molecules need to be targeted to the brain. One possible already developed strategy relies on the use of glucose derivatives leading to tri-functional compounds.⁵⁵

5.3. ABA derivatives in bi-functional acetyl-cholinesterase inhibitors

Designing bifunctional molecules for AD therapy becomes an interesting strategy. In addition to the BFC metal chelator described above, another class of bifunctional molecules has been recently developed, *i.e.* Bi-Functional AChE Inhibitor (BFI). They include an AChE inhibition moiety coupled to an ABA moiety. Indeed, in AD patients an important deficit in cholinergic neurons was observed, which leads to the "cholinergic hypothesis", according to which a low level of acetylcholine was responsible for cognitive and functional troubles observed in AD patients. Acetyl-cholinesterase inhibitors were thus strongly developed for AD treatment. They showed some positive effects on AD symptoms and are based on different scaffolds including tacrine, berberine, memoquin and rivastigmine (Fig. 5).

The first series of compounds synthesized are based on the memoquin scaffold, including a central a 2,5-diamino-benzoquinone core, linked to two BzT or ABT moieties, *via* diamine spacers ($n = 1$ or 4) (Fig. 5, 6–9).⁵⁶ These molecules have been evaluated for AChE inhibition and the activity of the bifunctional compounds was largely inferior to that of the memoquin, with only compound **9** showing a moderate activity ($IC_{50} = 0.305 \pm 0.009 \mu\text{M}$ versus 0.00155 ± 0.00011 for memoquin). In contrast but as expected the functionalized memoquin, in particular compound **6**, was slightly better in inhibition of A β 42 self-assembly, in line with a better cell viability of cells confronted with A β 42 oligomer-induced neurotoxicity observed in the presence of **6** compared to the memoquin only.

The same approach was pursued with tacrine or berberine entities as AChE inhibitors.⁵⁷ When evaluated using AChE inhibition assays, the berberine derivatives **27b** show comparable activity to that of the berberine moiety but a strongly

increased propensity to inhibit A β 42 aggregation. In contrast, the tacrine derivative **44b** showed a better AChE inhibition than the tacrine moiety but only a moderate inhibition of the A β 42 aggregation. The high AChE inhibition by **44b** was further investigated by molecular modelling and it was shown that the $n = 3$ spacer induced a better recognition with the enzyme, the tacrine moiety interacting with the central pocket and the ABT unit with a peripheral site.

More recently, the **BTC** and **BXC** compounds (Fig. 5) resulting from the structure of the **HBT** and **HBX** chelators, where the phenol moiety was linked to a carbamate function as a mimic of the active part of the rivastigmine inhibitor, were reported. In this strategy, the combination of a metal chelation moiety (that should be obtained after cleavage of the carbamate bond) and of an AChE inhibitor was expected to have a triple positive effect on metal chelation and A β targeting due to the ABT part (Section 5.2) and AChE inhibition due to the carbamate part. However, **BTC** and **BXC** revealed only very weak AChE inhibitors; although molecular modelling studies showed that **BTC** and to a lesser extent **BXC** occupy the same site than rivastigmine in line with the observed irreversible inhibition of the enzyme.⁵⁸

Only weak positive synergetic effects were detected in the above described studies, underlining the difficulty of combining several properties on a unique molecule. Further efforts are thus needed in this direction.

6. Concluding remarks

In the present review, we have highlighted the use of the benzazole scaffold and more particularly of its 2-arylbenzothiazole derivatives (ABT) as a SWAT ("Special Weapons and Tactics") to combat AD. Synthetic routes to 2-arylbenzazoles, including 2-arylbenzoxazoles and 2-arylbenzimidazoles, are now well-documented. It is anticipated that the easy access to these latter compounds in addition to the currently more investigated ABT will enlarge the possibility of substituent variations on the aromatic rings. This will thus lead to a new series of compounds for AD diagnosis and therapy.

Main applications of such organic scaffolds include the development of bi-functional compounds targeting multiple factors associated with AD (A β aggregation, metal ions, acetylcholinesterase, *etc.*). While the strategy relying on having only one molecule for multiple targets is highly appealing, the first results clearly show that such a strategy is far from being straightforward. Indeed and in line with the intrinsic complexity of such a disease, indirect or undesired effects have been observed leading for instance to an induction of a higher cytotoxicity by the compounds. This is particularly obvious for the bi-functional chelators, which instead of disassembling A β fibrils into non-toxic monomers induce the formation of highly toxic soluble A β oligomeric species. In line with the latter observation, the "oligomeric" issue appears here as central and key for the development of more efficient molecules, regardless of their potential applications (for understanding, diagnosing or curing AD). Hence, it is anticipated here that such oligomeric species will be one of the most attractive

targets in the near future and that efforts will be dedicated to better (i) characterize them *in vitro*, (ii) image them *in vivo* and (iii) target them for curative purposes.

Acknowledgements

We thank Prof. P. Faller for valuable discussions. Funding from the Région Midi-Pyrénées (S. N.) and from ANR Bobo (ANR-12-BS07-0005-01) is acknowledged.

References

- D. M. Holtzman, J. C. Morris and A. M. Goate, *Sci. Transl. Med.*, 2011, **3**, 77sr71.
- J. H. Viles, *Coord. Chem. Rev.*, 2012, **256**, 2271–2284.
- D. Valensin, C. Gabbiani and L. Messori, *Coord. Chem. Rev.*, 2012, **19–20**, 2357–2366.
- J. L. Hickey and P. S. Donnelly, *Coord. Chem. Rev.*, 2012, **256**, 2367–2380.
- C. Hureau, *Coord. Chem. Rev.*, 2012, **256**, 2164–2174.
- R. Kumar, U. Kalidhar, A. Kaur and J. Bajaj, *Res. J. Pharm., Biol. Chem. Sci.*, 2012, **3**, 166–178.
- A. A. Weekes and A. D. Westwell, *Curr. Med. Chem.*, 2009, **16**, 2430–2440.
- M. Cui, M. Ono, H. Kimura, M. Ueda, Y. Nakamoto, K. Togashi, Y. Okamoto, M. Ihara, R. Takahashi, B. Liu and H. Saji, *J. Med. Chem.*, 2012, **55**, 9136–9145.
- V. Facchinetti, R. d. R. Reis, C. R. B. Gomes and T. R. A. Vasconcelos, *Mini-Rev. Org. Chem.*, 2012, **9**, 44–53.
- V. N. Bochatay, P. J. Boissarie, J. A. Murphy, C. J. Suckling and S. Lang, *J. Org. Chem.*, 2013, **78**, 1471–1477.
- Y. Cheng, J. Yang, Y. Qu and P. Li, *Org. Lett.*, 2012, **14**, 98–101.
- G. Brasche and S. L. Buchwald, *Angew. Chem., Int. Ed.*, 2008, **47**, 1932–1934.
- P. Saha, T. Ramana, N. Purkait, M. A. Ali, R. Paul and T. Punniyamurthy, *J. Org. Chem.*, 2009, **74**, 8719–8725.
- J. Bonnamour and C. Bolm, *Org. Lett.*, 2008, **10**, 2665–2667.
- C. Praveen, K. H. Kumar, D. Muralidharan and P. T. Perumal, *Tetrahedron*, 2008, **64**, 2369–2374.
- M. M. Guru, M. A. Ali and T. Punniyamurthy, *J. Org. Chem.*, 2011, **76**, 5295–5308.
- M. Shen and T. G. Driver, *Org. Lett.*, 2008, **10**, 3367–3370.
- S. Ranjit and X. Liu, *Chem.–Eur. J.*, 2011, **17**, 1105–1108.
- A. Sharma, D. Vacchani and E. Van der Eycken, *Chem.–Eur. J.*, 2013, **19**, 1158–1168.
- K. Xie, Z. Yang, X. Zhou, X. Li, S. Wang, Z. Tan, X. An and C.-C. Guo, *Org. Lett.*, 2010, **12**, 1564–1567.
- G. Wu, J. Zhou, M. Zhang, P. Hu and W. Su, *Chem. Commun.*, 2012, **48**, 8964–8966.
- H. Bonin, R. Leuma Yona, B. Marchiori, P. Demonchaux and E. Gras, *Tetrahedron Lett.*, 2011, **52**, 1132–1135.
- N. Liu and Z.-X. Wang, *J. Org. Chem.*, 2011, **76**, 10031–10038.
- R. Leuma Yona, S. Mazères, P. Faller and E. Gras, *Chem-MedChem*, 2008, **3**, 63–66.
- R. J. Perry and B. D. Wilson, *Organometallics*, 1994, **13**, 3346–3350.
- T. B. Nguyen, L. Ermolenko, W. A. Dean and A. Al-Mourabit, *Org. Lett.*, 2012, **14**, 5948–5951.
- A. Kumar, S. Sharma and R. A. Maurya, *Tetrahedron Lett.*, 2010, **51**, 6224–6226.
- Y. Endo and J.-E. Bäckvall, *Chem.–Eur. J.*, 2012, **18**, 13609–13613.
- M. Biancalana and S. Koide, *Biochim. Biophys. Acta*, 2010, **1804**, 1405–1412.
- N. Amdursky, Y. Erez and D. Huppert, *Acc. Chem. Res.*, 2012, **45**, 1548–1557.
- A. A. Reinke and J. E. Gestwicki, *Chem. Biol. Drug Des.*, 2011, **77**, 399–411.
- L. P. Jameson, N. W. Smith and S. V. Dzyuba, *ACS Chem. Neurosci.*, 2012, **3**, 807–819.
- A. J. Veloso, V. W. S. Hung, G. Sindhu, A. Constantinof and K. Kerman, *Anal. Chem.*, 2009, **81**, 9410–9415.
- I. M. Kuznetsova, A. I. Sulatskaya, V. N. Uversky and K. K. Turoverov, *Mol. Neurobiol.*, 2012, **45**, 488–498.
- F. Mito, T. Yamasaki, Y. Ito, M. Yamato, H. Mino, H. Sadasue, C. Shirahama, K. Sakai, H. Utsumi and K.-i. Yamada, *Chem. Commun.*, 2011, **47**, 5070.
- O. Querbes, F. Aubry, J. Pariente, J. A. Lotterie, J. F. Demonet, V. Duret, M. Puel, I. Berry, J. C. Fort and P. Celsis, *Brain*, 2009, **132**, 2036–2047.
- G. R. Morais, A. Paulo and I. Santos, *Eur. J. Org. Chem.*, 2011, 1279–1293.
- W. E. Klunk, Y. Wang, G. F. Huang, M. L. Debnath, D. P. Holt and C. A. Mathis, *Life Sci.*, 2001, **69**, 1471–1484.
- B. C. Lee, J. S. Kim, B. S. Kim, J. Y. Son, S. K. Hong, H. S. Park, B. S. Moon, J. H. Jung, J. M. Jeong and S. E. Kim, *Bioorg. Med. Chem.*, 2011, **19**, 2980–2990.
- B. Neumaier, S. Deisenhofer, C. Sommer, C. Solbach, S. N. Reske and F. Mottaghy, *Appl. Radiat. Isot.*, 2010, **68**, 1066–1072.
- K. Serdons, T. Verduyck, D. Vanderghinste, P. Borghgraef, J. Cleynhens, F. Van Leuven, H. Kung, G. Bormans and A. Verbruggen, *Eur. J. Med. Chem.*, 2009, **44**, 1415–1426.
- G. Henriksen, A. I. Hauser, A. D. Westwell, B. H. Yousefi, M. Schwaiger, A. Drzezga and H.-J. r. Wester, *J. Med. Chem.*, 2007, **50**, 1087–1089.
- K. Serdons, C. Terwinghe, P. Vermaelen, K. Van Laere, H. Kung, L. Mortelmans, G. Bormans and A. Verbruggen, *J. Med. Chem.*, 2009, **52**, 1428–1437.
- C. A. Mathis, Y. Wang, D. P. Holt, G.-F. Huang, M. L. Debnath and W. E. Klunk, *J. Med. Chem.*, 2003, **46**, 2740–2754.
- Y. Wang, C. A. Mathis, G.-F. Huang, M. L. Debnath, D. P. Holt, L. Shao and W. E. Klunk, *J. Mol. Neurosci.*, 2003, **20**, 255–260.
- A. Lockhart, J. R. Lamb, T. Osredkar, L. I. Sue, J. N. Joyce, L. Ye, V. Libri, D. Leppert and T. G. Beach, *Brain*, 2007, **130**, 2607–2615.
- J. Pan, N. S. Mason, M. L. Debnath, C. A. Mathis, W. E. Klunk and K. S. Lin, *Bioorg. Med. Chem. Lett.*, 2013, **23**, 1720–1726.

- 48 S. Alavez, M. C. Vantipalli, D. J. S. Zucker, I. M. Klang and G. J. Lithgow, *Nature*, 2011, **472**, 226–229.
- 49 C. Rodríguez-Rodríguez, M. Telpoukhovskaia and C. Orvig, *Coord. Chem. Rev.*, 2012, **256**, 2308–2332.
- 50 A. Dedeoglu, K. Cormier, S. Payton, K. A. Tseitlin, J. N. Kremsky, L. Lai, X. Li, R. D. Moir, R. E. Tanzi, A. I. Bush, N. W. Kowall, J. T. Rogers and X. Huang, *Exp. Gerontol.*, 2004, **39**, 1641–1649.
- 51 A. K. Sharma, S. T. Pavlova, J. Kim, D. Finkelstein, N. J. Hawco, N. P. Rath, J. Kim and L. M. Mirica, *J. Am. Chem. Soc.*, 2012, **134**, 6625–6636.
- 52 Y. Zhang, L.-Y. Chen, W.-X. Yin, J. Yin, S.-B. Zhang and C.-L. Liu, *Dalton Trans.*, 2011, **40**, 4830.
- 53 C. Rodríguez-Rodríguez, N. S. de Groot, A. Rimola, A. n. Álvarez-Larena, V. Lloveras, J. Vidal-Gancedo, S. Ventura, J. Vendrell, M. Sodupe and P. González-Duarte, *J. Am. Chem. Soc.*, 2009, **131**, 1436–1451.
- 54 J. Geng, M. Li, L. Wu, J. Ren and X. Qu, *J. Med. Chem.*, 2012, **55**, 9146–9155.
- 55 L. E. Scott, M. Telpoukhovskaia, C. Rodríguez-Rodríguez, M. Merkel, M. L. Bowen, B. D. G. Page, D. E. Green, T. Storr, F. Thomas, D. D. Allen, P. R. Lockman, B. O. Patrick, M. J. Adam and C. Orvig, *Chem. Sci.*, 2011, **2**, 642–648.
- 56 M. L. Bolognesi, M. Bartolini, A. Tarozzi, F. Morroni, F. Lizzi, A. Milelli, A. Minarini, M. Rosini, P. Hrelia, V. Andrisano and C. Melchiorre, *Bioorg. Med. Chem. Lett.*, 2011, **21**, 2655–2658.
- 57 L. Huang, T. Su, W. Shan, Z. Luo, Y. Sun, F. He and X. Li, *Bioorg. Med. Chem.*, 2012, 1–11.
- 58 M. A. Telpoukhovskaia, B. O. Patrick, C. Rodríguez-Rodríguez and C. Orvig, *Mol. BioSyst.*, 2013, **9**, 792–805.